Probing the General Base Catalysis in the First Step of *Bam*HI Action by Computer Simulations†

Monika Fuxreiter‡ and Roman Osman*

Department of Physiology and Biophysics, Mount Sinai School of Medicine, New York, New York 10029

Received May 15, 2001; Revised Manuscript Received August 15, 2001

ABSTRACT: *Bam*HI is a type II restriction endonuclease that catalyzes the scission of the phoshodiester bond in the GAGTCC cognate sequence in the presence of two divalent metal ions. The first step of the reaction is the preparation of water for nucleophilic attack by Glu-113, which has been proposed to abstract the proton from the attacking water molecule. Alternatively, the 3′-phosphate group to the susceptible phosphodiester bond has been suggested to play a role as the general base. The two hypotheses have been tested by computer simulations using the semiempirical protein dipoles Langevin dipoles (PDLD/S) method. Deprotonation of water by Glu-113 has been found to be less favorable by 5.7 kcal/mol than metal-catalyzed deprotonation with a concomitant proton transfer to bulk solvent. The preparation of the nucleophile by the 3′-phosphate group is less favorable by 12.3 kcal/mol. These results suggest that both the general base and the substrate-assisted mechanisms in the first step of *Bam*HI action are less likely than the metal-catalyzed reaction. The metal ions in the active site of *Bam*HI make the largest contributions to the reduction of the free energy of hydroxide ion formation. On the basis of these findings we propose that the first step of endonuclease catalysis does not require a general base; rather, the essential attacking nucleophile in *Bam*HI catalytic action is stabilized by the metal ions.

Type II restriction endonucleases are part of the restriction modification system in bacteria (*1*, *2*). These enzymes cleave an invading phage DNA within a specific recognition sequence. The host DNA is protected from hydrolysis by methylation (*3*). Recognition of a specific sequence in the foreign DNA is therefore of vital importance for the survival of bacterial cells. Restriction endonucleases recognize a 4−8 base pair long palindromic DNA sequence with remarkably high specificity (*4*). Replacement of a single base pair often decreases the catalytic efficiency by as much as a millionfold.

The catalytic activity of *Bam*HI involves the scission of the phosphodiester bond in the GAGTCC cognate sequence, resulting in a 5′-phosphate and a free 3′-hydroxyl group (*5*). This reaction comprises three steps: (i) preparation of the attacking nucleophilic hydroxide by deprotonation, (ii) nucleophilic attack on the susceptible phosphate leading to the formation of a pentavalent intermediate/transition state, and (iii) dissociation of the 3′-leaving group. Each step requires assistance by a specific group: step i requires a general base to deprotonate the attacking water molecule; step ii needs a Lewis acid to stabilize the negatively charged pentavalent transition state, and step iii requires a general acid to protonate the 3′-hydroxy leaving group. To elucidate the mechanism of the enzymatic reaction, these groups have to be identified. The active site of type II restriction endonucleases contains four residues, usually three acidic groups and a lysine (*6*), which could potentially play a role as the necessary stabilizing groups. The active site of *Bam*HI is unique with four carboxylic residues, including a glutamate in the place of the lysine (*7*). Despite extensive biochemical and crystallographic studies, the role of the active site groups in endonuclease action has not been unequivocally elucidated.

The catalysis by *Bam*HI, similarly to all other restriction endonucleases, depends ultimately on the presence of divalent metal ions (*5*). However, due to ambiguity in the metal sites observed by X-ray crystallography (*8*−*11*), the function of these ions is not fully understood. Three models for the role of metal ions have been proposed, depending on the number of metal ions involved in catalysis.

In the *substrate-assisted model* one metal ion is required for catalysis. In this mechanism, the 3′-phosphate group to the scissile bond is proposed to deprotonate the attacking water molecule (*12*). The role of the metal ion in this model is to stabilize the additional negative charge that develops in the pentavalent transition state. The metal ion is also proposed to stabilize the OH^-, which is formed upon providing the necessary proton to the 3′-oxygen of the leaving group. The substrate-assisted mechanism conforms to kinetic data on modified substrates. Methyl phosphonate or phosphorothioate substitution of the 3′-phosphate group results in considerable decrease in cleavage activity (*13*, *14*). However, the O → S replacement affects the catalytic rate constant as far as four nucleotides from the cleaved bond (*14*). Furthermore, for the phosphate to act as a general base, its pK_a has to increase by ∼6 units from 0.76 (*15*). Such a large shift is not likely to occur in the presence of a divalent metal ion in the active site. These observations suggest a nonspecific electrostatic effect of the phosphates rather than a direct involvement in catalysis.

† M.F. acknowledges the support of OTKA Fellowship D 34572. This work was supported in part by USPHS Grant CA-63317.

* Corresponding author. Tel: (212) 241-5609. Fax: (212) 860-3369. E-mail: osman@inka.mssm.edu.

‡ Present address: Institute of Enzymology, H-1113 Budapest, Karolina ut 29, Hungary.

10.1021/bi010987x CCC: $20.00
Published on Web 10/31/2001

Another proposed mechanism requires *two metals* in the catalytic step. This mechanism was adapted from the exonuclease action of DNA polymerase I (*16*). The role of the metal ions was quantitatively analyzed, by comparing calculated activation barriers of different mechanisms to experimentally measured rate acceleration (*17*). This work provided a clear interpretation of the catalytic effect of metal ions. The metal ion in the proximity of the attacking nucleophile (metal ion A) lowers the pK_a of this water molecule by ~4 pH units by stabilizing the resulted OH^- ion. This metal ion was not found to reduce the orientational entropy of the nucleophile by providing angular constraints. The second metal ion (metal ion B) plays an important role in the nucleophilic attack step by stabilizing the developing negative charge on the pentavalent transition state. However, it has been shown that the catalytic effect of the second metal ion is not due to the preference of the metal for the pentavalent geometry of the transition state vs the tetrahedral geometry of the reactant. Rather, the dominance of electrostatic effects over entropy factors or strain has been clearly demonstrated.

The crystal structures of the pre- and postreactive complexes of *Bam*HI seem to support the two-metal mechanism (*10*). In the crystal structure of the prereactive complex of *Bam*HI, Glu-113 is hydrogen bonded to the putative attacking water molecule (*10*). Kinetic results show that mutations of Glu-113 to Cys or Gly decrease the enzymatic activity by 3 or 4 orders of magnitude, respectively (*18*). Replacement of Glu by Asp results in a 10-fold decrease in activity (*18*), whereas mutation of Glu-113 to Lys abolishes the enzymatic activity altogether (*19*). These results have been used to propose a role for Glu-113 as a general base. Although this mechanism seems to be a plausible explanation of *Bam*HI catalysis, it is not straightforward to extend it to other restriction endonucleases because Glu-113 in *Bam*HI is replaced by a Lys in other enzymes.

The third mechanism proposes the involvement of *three metal ions* in catalysis. This model recapitulates the two-metal pathway, assigning a structural role to the third metal ion (*11*, *20*). In addition, the third metal ion has been suggested to lower the pK_a of a bound water molecule, so that it can provide a proton to the leaving group. This hypothesis, however, is not supported by direct structural data.

Understanding the role of metal ions is therefore a central element in developing a unified mechanism for type II restriction endonucleases. In the present work, the role of metal ions has been investigated in the first step of *Bam*HI catalysis. We find that deprotonation of the nucleophilic water molecule by a general base or a substrate-assisted mechanism is unlikely. Instead, metal ion A makes the major contribution to reducing the free energy of hydroxide ion formation. Our work suggests that the role of metal ion A is primarily responsible for stabilizing the nucleophile.

METHODS

Models. The starting model for our calculations was constructed from the crystal structure of the prereactive complex of *Bam*HI (PDB ID: 2bam). The inhibitory Ca^{2+} ions at the active site were replaced with Mg^{2+} ions. Four crystallographic water molecules positioned within 5 Å from the scissile phosphate group were treated explicitly. All other water molecules were replaced by Langevin dipoles. The Langevin dipoles were constructed by immersing the protein in a 15 Å sphere that contained a cubic grid of 1 Å spacing and removing all of the points within a van der Waals distance from protein atoms. The remaining points were assigned an average polarization equivalent to that of a water molecule. A grid of Langevin dipoles with 3 Å spacing and a radius of 18 Å represented the outer part of the solvent. Residues within 6.5 Å from the scissile phosphate group were ionized. These include the active site residues Glu-77, Asp-94, and Glu-111, Mg^{2+}(A), Mg^{2+}(B), the susceptible phosphate group, and Arg-122. To test the role of Glu-113 as a general base catalyst, four models have been constructed with different ionization states of Glu-113 and the attacking water molecule (Figure 1). These models correspond to the reactant and product states of proton transfer reactions by various mechanisms. For example, structures **i** and **iv** are related by a direct proton transfer, whereas structure **ii** represents protonation of Glu-113 by an external (to this system) source of protons and structure **iii** represents a transfer of a proton from the water to an external source. The two models, **v** and **vi**, have been used to probe the substrate-assisted mechanism. Here the general base is the phosphate groups 3′ to the scissile bond.

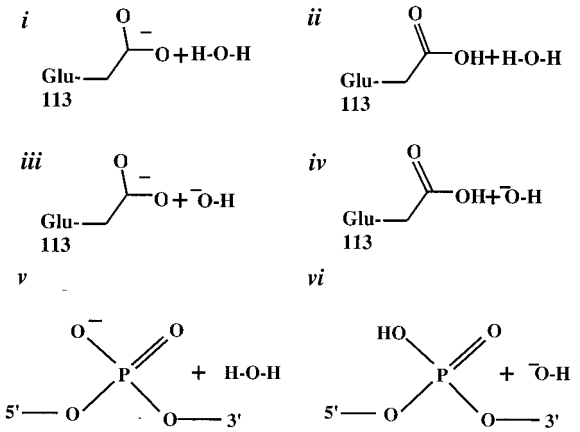

FIGURE 1: Charge configurations used for calculation of $\Delta\Delta G^{w\rightarrow p}$: (**i**−**iv**) configurations representing the general base and metal catalysis; (**v**, **vi**) configurations corresponding to substrate-assisted catalysis.

Calculation of the Free Energy of Proton Transfer. The energy of deprotonation of the attacking water molecule has been calculated with the formulation in eq 1, which is based on the thermodynamic cycle presented in Figure 2:

$$\Delta G^{p}(AH_p + B_p^- \rightarrow A_p^- + BH_p) = \Delta G^{w}(AH_w + B_w^- \rightarrow A_w^- + BH_w) - \Delta\Delta G^{w\rightarrow p}(AH + B^-) + \Delta\Delta G^{w\rightarrow p}(A^- + BH) \quad (1)$$

where

$$\Delta G^{p}(AH_p + B_p^- \rightarrow A_p^- + BH_p)$$

is the free energy of proton transfer from water to the general base in protein,

$$\Delta G^{w}(AH_w + B_w^- \rightarrow A_w^- + BH_w)$$

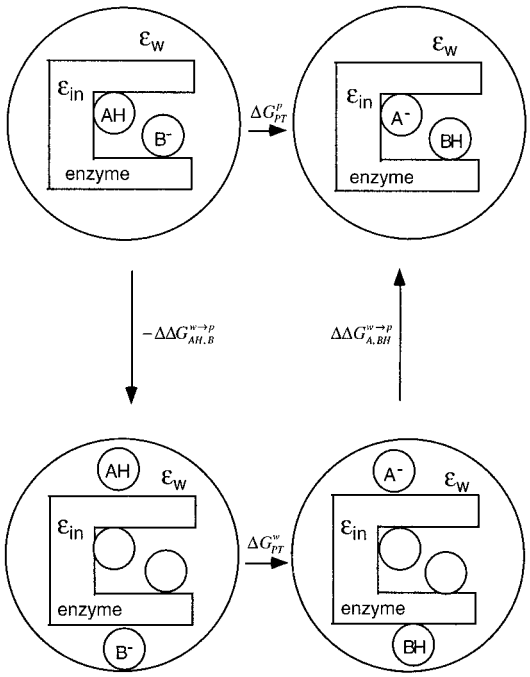

FIGURE 2: Thermodynamic cycle for calculating the free energy of proton transfer.

is the free energy of proton transfer from water to the general base in water,

$$\Delta\Delta G^{\mathrm{w}\rightarrow\mathrm{p}}(\mathrm{AH}+\mathrm{B}^{-})$$

is the free energy of moving the water molecule together with the ionized general base from water to the protein site, and

$$\Delta\Delta G^{\mathrm{w}\rightarrow\mathrm{p}}(\mathrm{A}^{-}+\mathrm{BH})$$

is the free energy of moving the hydroxide ion with the protonated general base from water to protein site.

The free energy differences of the reactive groups in water and in protein have been calculated according to eq 2, which is based on the semimicroscopic version of the protein dipoles Langevin dipoles model (PDLD/S) (Figure 3):

$$\Delta\Delta G^{\mathrm{w}\rightarrow\mathrm{p}}=[\sum_{i}-\Delta G^{i,\infty}_{\mathrm{sol,w}}+(\Delta G^{\mathrm{p}}_{\mathrm{sol,w}}(q=q_0)-\Delta G^{\mathrm{p}}_{\mathrm{sol,w}}(q=0))]\left(\frac{1}{\epsilon_{\mathrm{in}}}-\frac{1}{\epsilon_{\mathrm{w}}}\right)+V_{\mu q}\frac{1}{\epsilon_{\mathrm{in}}} \quad (2)$$

where $\sum_i -\Delta G^{i,\infty}_{\mathrm{sol,w}}$ is the solvation energy of the specific residue in water when the charged groups are infinitely separated from each other. $\Delta G^{\mathrm{p}}_{\mathrm{sol,w}}(q=q_0)$ and $\Delta G^{\mathrm{p}}_{\mathrm{sol,w}}(q=0)$ are the solvation energies of protein in water when the specific group is in charged and uncharged form (with zero residual charges), respectively. $V_{\mu q}$ is the interaction of the reactive groups with the protein charges and polar groups in a vacuum. ϵ_{w} is the dielectric constant of water, and ϵ_{in} is a scale factor that represents the contributions, which are not considered explicitly in the model. As the protein-induced dipoles and the reorganization of permanent dipoles to charge rearrangements were included implicitly, ϵ_{in} was set to be equal to 4 and was used throughout this work.

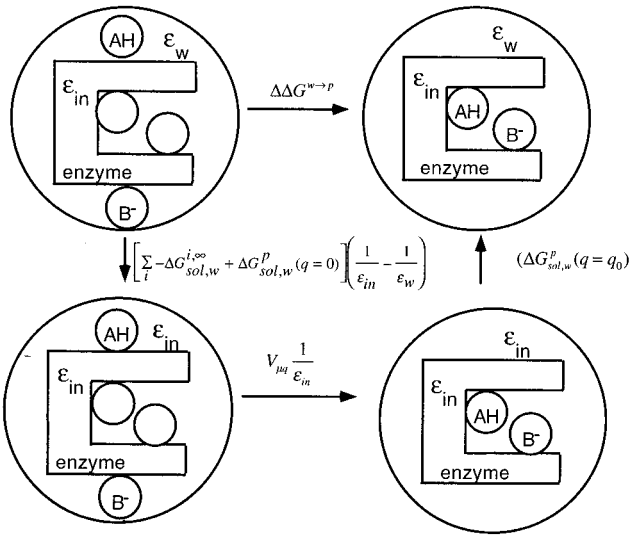

FIGURE 3: Thermodynamic cycle for calculating $\Delta\Delta G^{\mathrm{w}\rightarrow\mathrm{p}}$ of reactants and products by the PDLD/S method.

Structural reorganization was demonstrated to have a significant effect on the free energy of charge formation on a protein group (*21*, *22*). The effect of protein relaxation upon transferring the charged groups from water to the protein site has been taken into account by the linear response approximation (LRA) (*23*). The electrostatic free energies were averaged over protein configurations, as expressed in eq 3. The configurations for averaging were generated by molecular dynamics simulations with the reacting groups in charged and uncharged form, respectively:

$$\Delta\Delta G^{\mathrm{w}\rightarrow\mathrm{p}}=\frac{1}{2}(\langle\Delta\Delta G^{\mathrm{w}\rightarrow\mathrm{p}}\rangle_{q=q_0}+\langle\Delta\Delta G^{\mathrm{w}\rightarrow\mathrm{p}}\rangle_{q=0}) \quad (3)$$

where the $\langle\Delta\Delta G^{\mathrm{w}\rightarrow\mathrm{p}}\rangle_{q=q_0}$ is the average solvation energy of configurations generated when the relevant groups are charged and the $\langle\Delta\Delta G^{\mathrm{w}\rightarrow\mathrm{p}}\rangle_{q=0}$ term applies for uncharged configurations.

Simulation Details. The PDLD/S−LRA calculations have been performed with the surface constrained all atom solvent model (SCAAS) (*24*). In the SCAAS approximation the protein/solvent system is divided into four regions: region I contains the attacking water molecule and the group that is tested as the general base, Glu-113 or the 3′-phosphate group to the scissile bond (see Figure 1). The rest of the protein is assigned to region II, where all atoms are treated explicitly. Region III is defined by the Langevin grid of the solvent truncated to a sphere with a grid spacing of 1 Å in the proximity of region I and of 3 Å in the outer part (see above). Region IV represents the bulk solvent, which is treated by a macroscopic continuum approximation.

The PDLD/S−LRA calculations were performed with the program POLARIS 6.30, using the ENZYMIX force field for MD simulations (*23*). To compute electrostatic free energies in conformations that are close to the crystal structure, the initial models were only relaxed for 5 ps during MD simulations at 300 K. $\Delta\Delta G^{\mathrm{w}\rightarrow\mathrm{p}}$ of the reactive groups, which were included in region I, has been obtained by averaging the results of 10 configurations, each generated in 2 ps MD simulations. The $\Delta\Delta G^{\mathrm{w}\rightarrow\mathrm{p}}$ values converged after 6−8 configurations.

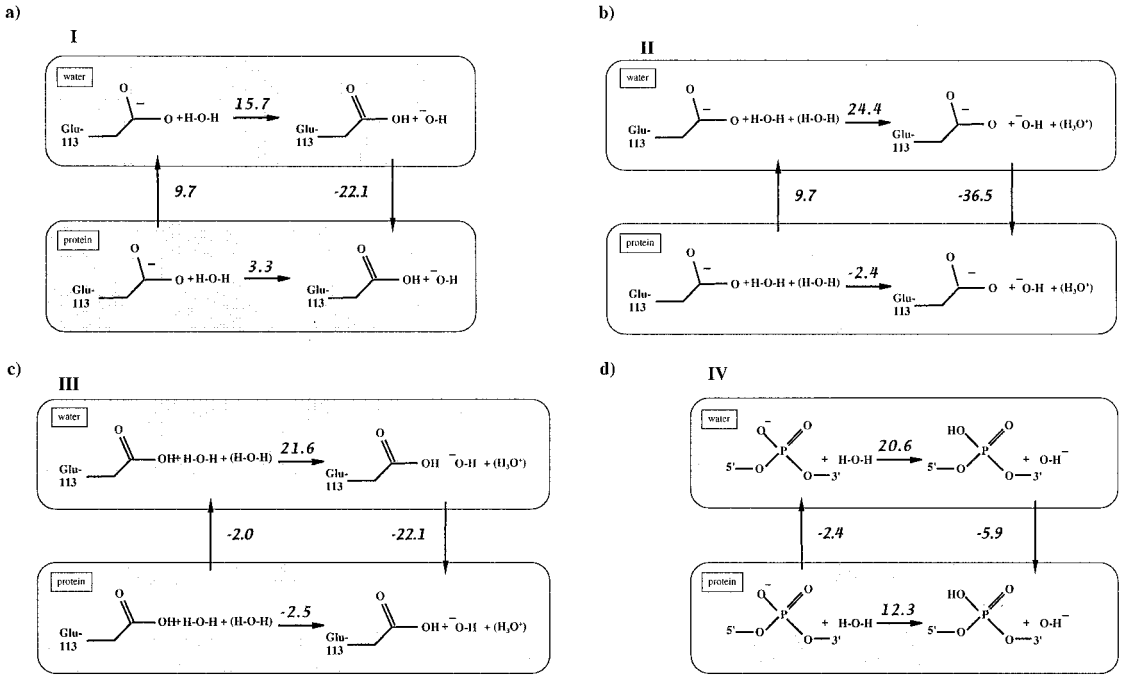

FIGURE 4: Thermodynamic cycles for free energy calculations of the proton transfer processes by four possible reaction mechanisms. The thermodynamic cycles are constructed as described in Figure 2. (a) Mechanism I, general base catalysis. (b) Mechanism II, metal catalysis in the presence of ionized Glu-113. (c) Mechanism III, metal catalysis in the presence of neutral Glu-113. (d) Mechanism IV, substrate-assisted mechanism.

Evaluation of Group Contributions. To evaluate the energetic contributions of individual residues to the free energy, we have applied the so-called "nonrelaxed" approximation (*25*). In this approach, the contribution of an individual residue is estimated as the free energy difference between the stabilization of region I when the particular residue is charged and in fully nonpolar form (with zero residual charges). In the process of the charge annihilation of a given group, the protein structure and the explicit solvent molecules are not allowed to relax. For polar but not ionized residues the $V_{\mu q}/\epsilon_{in}$ term (eq 2) was found to give the major contribution. This term is the interaction between the charges of the reacting system and the residual charges of the protein scaled by the factor ϵ_{in}, which accounts for the implicit dielectric screening in the model. Previous studies on analogous systems established the appropriate values for ϵ to be used in such calculations (*25*). Accordingly, $\epsilon_{in} = 4$ was used for polar groups and $\epsilon_{in} = 40$ for ionized groups. The group contributions for first-shell residues of the group of interest obtained by the nonrelaxed approximation were shown to be in good agreement with the group contributions obtained by the relaxed approach (*26*).

RESULTS AND DISCUSSION

To examine the mechanism of water deprotonation in *Bam*HI, the four reactions (I−IV) presented in Figure 4 have been studied. For each mechanism the thermodynamic cycle (described in Figure 2) is displayed, where the upper part corresponds to the reaction in water and the lower part represents the same reaction mechanism in protein. In mechanism I (Figure 4a), Glu-113 acts as a general base, which deprotonates the hydrogen-bonded water molecule preparing the attacking nucleophile. In mechanisms II and III (Figure 4b,c), another water molecule plays the role of accepting the proton from the attacking water molecule. The latter two mechanisms represent the metal-catalyzed reaction in the presence of two different states of Glu-113. Because the putative nucleophilic water is also bound to the metal ion, these models test whether the catalysis of proton transfer to a second water molecule, which is assumed to be in direct contact with the bulk phase, is affected by the ionization state of Glu-113, charged in mechanism II and neutral in mechanism III. The "spectator" water molecule (in parentheses), because of its connection to bulk, was not considered explicitly in the simulation, but its effect is felt through the Langevin field of the continuum and the intrinsic energy of transferring a proton from a water molecule to bulk (water dissociation). Mechanism IV (Figure 4d) corresponds to the substrate-assisted reaction, in which the 3′-phosphate deprotonates the water that participates in the nucleophilic attack on the scissile bond.

Calculation of the free energies of the proton transfer processes in protein (based on the thermodynamic cycle presented in Figure 2) requires the evaluation of the free energy of the respective reaction in water [$\Delta G_w(H_2O + B^- \rightarrow OH^- + BH)$] as well as the free energies of moving the reactants and products from water to the protein site [$\Delta\Delta G^{w\rightarrow p}(H_2O + B^-)$].

The free energies of the corresponding reference reactions in water were obtained from the experimental pK_a values:

$$\Delta G^w(H_2O_w + B_w^- \rightarrow OH_w^- + B - H_w) = 2.3RT[pK_a(H_2O)_w - pK_a(B - H)_w] \quad (4)$$

The calculated free energies in aqueous solutions, when the reactants are in the same solvent cage, are summarized in Table 1. As expected from the comparison of the corresponding pK_a values, the proton transfer from water to glutamate is found to be the most favorable mechanism in solution. Proton transfer from water to the phosphate requires

Table 1: Free Energies of the Reference Reactions in Water

reaction	ΔG^{w}_{PT} (kcal/mol)
$Glu\text{-}COO^- + H_2O \rightarrow Glu\text{-}COOH + OH^-$ (I)	15.8[a]
$(Glu\text{-}COO^-) + H_2O + H_2O \rightarrow (Glu\text{-}COO^-) + OH^- + H_3O^+$ (II)	24.4[b]
$(Glu\text{-}COOH) + H_2O + H_2O \rightarrow (Glu\text{-}COOH) + OH^- + H_3O^+$ (III)	21.6
$P(OH)_2O_2^- + H_2O \rightarrow P(OH)_3O + OH^-$ (IV)	20.6[c]

[a] Considering standard conditions, 1 M H_2O and 1 M Glu-COOH (reactants are in the same solvent cage). [b] Glu-COO^- and OH^- are assumed to be in the same solvent cage. We estimate the electrostatic repulsion between the charged groups separated at $r = 2.9$ Å (as in the crystal structure of the prereactive complex) and $\epsilon = 40$ to be 2.8 kcal/mol. [c] The pK_a of 0.76 was used for the $P(OH)_2O_2^-$ (*15*).

Table 2: $\Delta\Delta G^{w\rightarrow p}$ of Reactant and Product Models

structure	$\Delta\Delta G^{w\rightarrow p}$ (kcal/mol)	structure	$\Delta\Delta G^{w\rightarrow p}$ (kcal/mol)
i	−9.7	**iv**	−22.1
ii	2.0	**v**	2.4
iii	−36.5	**vi**	−5.9

an additional 4.8 kcal/mol, compared to the neutralization of glutamate by water. The hypothetical process of transferring a proton between two water molecules in the presence of glutamic acid in the same solvent cage is the least favorable reaction, which requires 2.8 kcal/mol more than the proton transfer to phosphate.

The free energies of transferring the reactants and products (models **i**−**vi** in Figure 1) from water to the protein are displayed in Table 2. In the reactant models, the ionized Glu-113 with a neutral water molecule (model **i**) are stabilized in the protein environment by 9.7 kcal/mol, whereas the protonated Glu-113 (model **ii**) is destabilized by the protein compared to aqueous environment. The corresponding product models (**iii**, **iv**) that include the attacking nucleophile show a marked stabilization by the protein of the deprotonated Glu-113 with an OH^-. However, while the protein stabilizes the neutralized Glu-113 with an OH^- compared to aqueous environment by 22.1 kcal/mol (model **iv**), the stabilization is considerably less than the corresponding model **iii** with the ionized Glu-113. Models of the substrate-assisted mechanism (**v**, **vi**) indicate that the protein environment, compared to aqueous environment, prefers the neutral phosphate with deprotonated water over the charged phosphate group with neutral water, albeit by a smaller amount.

Combining the results in Tables 1 and 2 into thermodynamic cycles gives the free energies of proton transfer in the enzyme by the four possible mechanisms (Figure 4). The thermodynamic cycles show that the most favorable process in the enzyme is the proton transfer from the attacking water to the spectator water molecule connected to bulk (mechanisms II and III). Since these mechanisms represent the effect of the metal on ionization of the bound water, this result demonstrates that the pK_a of the attacking water molecule is significantly lowered by the presence of the metal ion. In contrast, the formation of OH^- by general base catalysis (mechanism I) requires an additional 5.8−5.9 kcal/mol. It is important to note that these results are consistent with macroscopic calculations of the pK_a by the ESPOT program (*27*). This method accounts for the local environmental effects in the protein through screened Coulombic potentials and gives pK_a values of 3.2 for Glu-113 and 6.2 for the attacking water molecule. Interestingly, the energies of mechanisms II and III show that proton transfer is not sensitive to the ionization state of Glu-113. In the reactant state, however, the enzyme stabilizes the ionized Glu-113 with water by 9.7 kcal/mol compared to the aqueous environment and destabilizes the neutral Glu-113 by 2 kcal/mol (see Table 2). Thus, the mechanism involving the negatively charged Glu-113 is the preferred pathway.

If Glu-113 does not play the role of a general base, one might wonder what can cause the substantial rate decrease of upon mutating this residue (*28*). The substitution is E113K results in complete loss of enzymatic activity and an increase in affinity (*29*). It is possible that the replacement of Glu by Lys disrupts the metal site A, which can lead to severe changes in the catalytic mechanism because of the importance of metal A on catalysis (see below). All other known substitutions appear to only change the electrostatic effect of Glu-113, such that the effect on the metal ion as well as on the incoming water molecule can reduce the stabilization of the nucleophile in the mutant enzymes. Thus, on the basis of our calculations and the experimental results, we conclude that Glu-113 has an electrostatic effect on the *Bam*HI action rather than a direct involvement in catalysis as a general base. This is consistent with the conclusion from recent work (*29*).

The free energy of proton transfer from the attacking water to the 3′-phosphate group is reduced significantly in the enzyme compared to the reaction in the aqueous phase (Figure 4d). The free energy of this reaction is now only 12.3 kcal/mol. Nevertheless, this demonstrates that proton abstraction by the 3′-phosphate group to the susceptible phosphate is highly unlikely. On the basis of the free energies presented in Figure 4, mechanism II can be proposed as the proton transfer pathway in the enzyme.

To gain a better understanding of the factors that contribute to the stabilization of hydroxide ion by the protein, the contributions of individual residues in mechanism II have been analyzed. The nonrelaxed contributions (see Methods) were obtained by subtracting the corresponding $V_{\mu q}/\epsilon_{in}$ terms (eq 2, Methods) that represent the electrostatic interactions for the OH^- with the protein groups from those computed for the H_2O. We have selected to include the group contributions that are larger than 1 kcal/mol. The results are displayed in Figure 5.

The major stabilization of the hydroxide ion is provided by the metal ions in the active site of the enzyme. Metal ion A stabilizes the ionization of the attacking water by 7.8 kcal/mol, whereas metal ion B contributes only 3 kcal/mol. This suggests that replacing metal ion A by a neutral residue, e.g., by mutating the residue that anchors Mg^{2+}−A to a neutral residue, should decrease the rate of the reaction by ∼6 orders of magnitude. On the other hand, a similar substitution that will affect the binding of Mg^{2+}−B may only decrease the rate by 2 orders of magnitude. As far as we know, none of these replacements have been tested experimentally.

The prediction of reaction rates upon replacing the metal ions by a protein residue or another metal ion is complicated by many factors. One of the most important is the rearrangement of the protein upon such changes. Without actually performing the simulations to determine the changes in structure, or obtaining them from experimental data, the

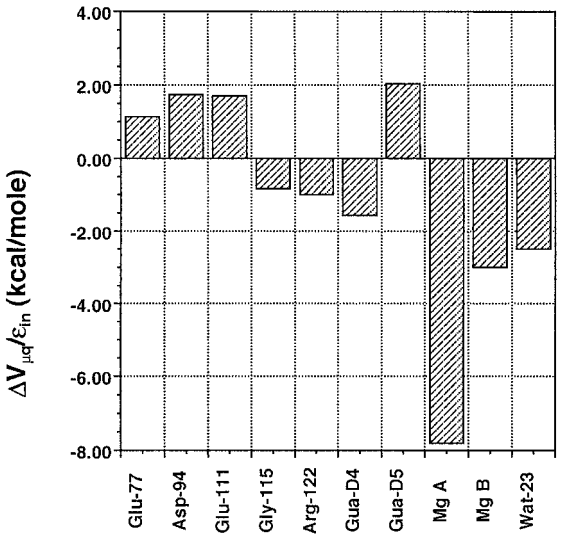

FIGURE 5: Group contributions to the free energy of OH^- relative to that of H_2O for mechanism II.

prediction is based on the assumption that the change in the structure upon metal replacement or mutation is sufficiently small to not affect the subtle balance between different energetic components. The effect of metal ion substitution on staphylococcal nuclease catalysis has been studied extensively by Åquist and Warshel (*30*). Their work demonstrated that the preference for a certain type of metal ion is determined by the dependence of two reaction steps—the preparation of the nucleophile and the nucleophilic attack on the stabilized pentavalent transition state—on the metal ion size. The stabilization of the doubly charged pentavalent transition state is more sensitive to ion size than the stabilization of the nucleophile. Therefore, predicting the overall rate of the *Bam*HI reaction on other metal ions based only on the quantified contributions of the metal ions to the first step in the phosphodiester bond hydrolysis lacks the balance between the two steps. A large decrease in the free energy of forming the nucleophile can make the nucleophilic attack step more difficult, i.e., potentially increasing the activation energy of the reaction. Predictions on the reaction rates with different metal ions using kinetic data on other restriction endonucleases are also not reliable due to the difference in composition and geometry of the active sites (*31*, *32*). Interestingly, another stabilization factor is a water molecule (water 23 in the crystal structure) at the active site, which is perfectly aligned to interact with the nucleophile. This water contributes 2.2 kcal/mol to the stabilization of the nucleophile primarily by a dipole−dipole electrostatic interaction. This water is important in the last stage of the reaction, providing a proton to the O3′ leaving group. A subtle stabilizing effect is generated by the N−H backbone dipoles of Gly-115 and Arg-122. They are positioned in close proximity to the OH^- and are perfectly aligned to stabilize the negative charge on the nucleophile.

The negatively charged active site groups, Glu-77, Asp-94, and Glu-111, contribute the major destabilization of the nucleophile. These are the residues that contribute to the binding of the metal ions, and their destabilization of the OH^- comes from a simple electrostatic repulsion between the negative charges. Another important group that destabilizes the nucleophile is the scissile phosphate group (Gua-D5). This is also a simple electrostatic repulsion, which has been well characterized, and the role of the metal ions in the overall energetic balance is therefore very important.

The phosphate−sugar backbone of the Gua-D4 in DNA stabilizes the OH^- by 1.5 kcal/mol. This is a long-range electrostatic interaction since there are no direct contacts between the backbone of Gua-D4 and either the water or the OH^-. This observation rationalizes why methyl phosphonate or phosphorothioate substitution of this phosphate groups results in considerable decrease in cleavage activity (*13*, *14*). However, such a conclusion should be considered with considerable caution because the present study only addresses the energetics of the formation of the nucleophile, whereas the investigations with the phosphate analogues measure a k_{cat}/K_M for the entire reaction which is affected by many steps including substrate binding and product release.

CONCLUSIONS

Four possible mechanisms for forming the nucleophile in *Bam*HI action have been probed by computer simulations. On the basis of the calculated free energies, the general base catalysis is an unlikely mechanism for deprotonation of the attacking water molecule. The substrate-assisted mechanism, which involves transferring the proton to the phosphate group 3′ to the susceptible phosphate, was concluded to be even less probable. Our results show that metal ion A plays a crucial role in the proton transfer reaction, providing the major stabilization of the nucleophile. Metal ion B is less important, although it has the second largest contribution to the stabilization of the hydroxide ion formation. Interestingly, the water molecule bound to metal ion B is also an energetic factor in this reaction. These results suggest that site B does not have as rigorous a requirement for stabilization as the metal in site A and could possibly be replaced by another positively charged group.

General base catalysis is not always the most effective way to reduce the barrier in reactions that involve OH^-. For example, in DNA polymerase I the computed free energy in a catalytic step with an external OH^- has been shown to agree with experimental results better than the potential hydroxide produced in general base catalysis by Glu-357 (*17*). The two metal ions in DNA polymerase I have been found to catalyze different steps of the phosphodiester bond hydrolysis. The first ion stabilizes the negative charge of the nucleophile, while the second one assists in the nucleophilic attack by helping in the migration of the negative charge from the nucleophile to the phosphate. The computer simulations on the formation of the nucleophile in *Bam*HI presented in this work support this two-metal mechanism.

The observation that Glu-113 does not play the role of a general base in the first step of *Bam*HI catalysis serves as the basis for proposing a general mechanistic scheme for type II restriction endonucleases. The equivalent position of Glu-113 in *Bam*HI is occupied by a Lys other restriction endonucleases. The lysine has been proposed to deprotonate the attacking water molecule by acting as a general base, in analogy to the proposed role of Glu-113 in *Bam*HI. For an effective general base catalysis the lysine has to be in a neutral state, but it is very difficult to rationalize the lowering of its pK_a in the presence of a highly ionized active site and in the proximity of the negatively charged backbone of the

DNA. Hence we propose that the first step in the endonuclease catalysis in *Bam*HI is carried out with the assistance of an external water molecule, whose deprotonation is induced by the metal ion rather than by a general base. The major energetic factor in this reaction step is the stabilization of the nucleophile derived from the water by the neighboring metal ion.

REFERENCES

1. Wilson, G. G., and Murray, N. E. (1991) *Annu. Rev. Genet. 25*, 585−627.
2. Wilson, G. G. (1991) *Nucleic Acids Res. 19*, 2539−2566.
3. Heitman, J. (1993) in *Genetic engineering* (Setlow, J. K., Ed.) pp 57−108, Plenum Press, New York.
4. Roberts, R. J., and Halford, S. E. (1993) in *Nucleases* (Linn, S. M., Lloyd, R. S., and Roberts, R. J., Eds.) pp 35−88, Cold Spring Harbor Laboratory Press, Cold Spring Harbor, NY.
5. Pingoud, A., and Jeltsch, A. (1997) *Eur. J. Biochem. 246*, 1−22.
6. Aggarwal, A. K. (1995) *Curr. Opin. Struct. Biol. 5*, 11−19.
7. Newman, M., Strzelecka, T., Dorner, L. F., Schildkraut, I., and Aggarwal, A. K. (1994) *Nature 368*, 660−664.
8. Kostrewa, D., and Winkler, F. K. (1995) *Biochemistry 34*, 683−696.
9. Perona, J. J., and Martin, A. M. (1997) *J. Mol. Biol. 273*, 207−225.
10. Viadiu, H., and Aggarwal, A. K. (1998) *Nat. Struct. Biol. 5*, 910−916.
11. Horton, J. R., Nastri, H. G., Riggs, P. D., and Cheng, X. (1998) *J. Mol. Biol. 284*, 1491−504.
12. Jeltsch, A., Alves, J., Maass, G., and Pingoud, A. (1992) *FEBS Lett. 304*, 4−8.
13. Jeltsch, A., Pleckaityte, M., Selent, U., Wolfes, H., Siksnys, V., and Pingoud, A. (1995) *Gene 157*, 157−162.
14. Thorogood, H., Grasby, J. A., and Connolly, B. A. (1996) *J. Biol. Chem. 271*, 8855−8862.
15. Guthrie, J. P. (1977) *J. Am. Chem. Soc. 99*, 3991−4000.
16. Beese, L. S., and Steitz, T. A. (1991) *EMBO J. 10*, 25−33.
17. Fothergill, M., Goodman, M. F., Petruska, J., and Warshel, A. (1995) *J. Am. Chem. Soc. 117*, 11619−11627.
18. Bitinaite, J., Wah, D. A., Aggarwal, A. K., and Schildkraut, I. (1998) *Proc. Natl. Acad. Sci. U.S.A. 95*, 10570−10575.
19. Xu, S.-Y., and Schildkraut, I. (1991) *J. Bacteriol. 173*, 5030−5035.
20. Horton, N. C., Newberry, K. J., and Perona, J. J. (1998) *Proc. Natl. Acad. Sci. U.S.A. 95*, 13489−13494.
21. Sham, Y. Y., Muegge, I., and Warshel, A. (1998) *Biophys. J. 74*, 1744−1753.
22. Fuxreiter, M., Warshel, A., and Osman, R. (1999) *Biochemistry 38*, 9577−9589.
23. Lee, F. S., Chu, Z. T., and Warshel, A. (1993) *J. Comput. Chem. 14*, 161−185.
24. King, G., and Warshel, A. (1989) *J. Chem. Phys. 91*, 3647−3661.
25. Muegge, I., Schweins, T., Langen, R., and Warshel, A. (1996) *Structure 4*, 475−489.
26. Muegge, I., Tao, H., and Warshel, A. (1997) *Protein Eng. 10*, 1363−1372.
27. Mehler, E. L., and Guarnieri, F. (1999) *Biophys. J. 75*, 3−22.
28. Dorner, L. F., and Schildkraut, I. (1994) *Nucleic Acids Res. 22*, 1068−1074.
29. Engler, L. E., Sapienza, P., Dorner, L. F., Kucera, R., Schildkraut, I., and Jen-Jacobson, L. (2001) *J. Mol. Biol. 307*, 619−636.
30. Åquist, J., and Warshel, A. (1990) *J. Am. Chem. Soc. 112*, 2860−2868.
31. Baldwin, G. S., Sessions, R. B., Erskine, S. G., and Halford, S. (1999) *J. Mol. Biol. 288*, 87−103.
32. Horton, J. R., and Cheng, X. (2000) *J. Mol. Biol. 300*, 1049−1056.

BI010987X